Available online at www.sciencedirect.com
SCIENCE DIRECT
Materials Chemistry and Physics 94 (2005) 347–352
MATERIALS CHEMISTRY AND PHYSICS
www.elsevier.com/locate/matchemphys

The influence of yttrium on a typical SnO_2 varistor system: Microstructural and electrical features

R. Parra [a,*], Y. Maniette [b], J.A. Varela [b], M.S. Castro [a]

[a] *Instituto de Investigaciones en Ciencia y Tecnología de Materiales (INTEMA, CONICET-UNMdP), J.B. Justo 4302, B7608FDQ - Mar del Plata, Argentina*
[b] *Instituto de Química, UNESP, PO Box 355, 14801-970 Araraquara, SP, Brazil*

Received 28 December 2004; received in revised form 19 April 2005; accepted 10 May 2005

Abstract

The influence of yttrium oxide, Y_2O_3, on the microstructure development of the $SnO_2{\cdot}Co_3O_4{\cdot}Nb_2O_5$ typical varistor system was studied with scanning (SEM) and transmission (TEM) electron microscopies. The different phases present in the studied samples were characterized through XRD, EDS and selected area diffraction patterns (SAD). Particles of Co_2SnO_4 were observed with TEM in every sample, whereas clusters of the pyrochlore phase$Y_2Sn_2O_7$ were observed with SEM in samples with 0.05, 0.10 and 0.25 mol% of Y_2O_3. The higher non-linearity ($\alpha = 16$) was achieved with the addition of 0.05 mol% of Y_2O_3. The influence of the secondary phases on the electrical properties is also addressed in this work.

Keywords: Varistors; Electron microscopy; Electrical properties; SnO_2

1. Introduction

Metal oxide varistors are electroceramic devices commonly used as surge arrestors in electronic circuits and power systems. They can be used over wide ranges of voltages and currents according to their specific properties. The most widely studied class of varistor is manufactured by sintering ZnO with small additions of metal oxides such as CoO, Bi_2O_3, Sb_2O_3 and MnO [1–3]. The resultant product is a polycrystalline ceramic in which spinel and pyrochlore phases may be present [4,5]. These devices exhibit highly non-linear voltage–current characteristics by virtue of which they act as insulators or conductors depending on the applied voltage. Thermionic emission and tunnelling are acknowledged to be the major charge carrier transport mechanisms [6].

A new varistor system based on SnO_2 has been introduced by Pianaro et al. in 1995 [7]. The simple microstructure, consisting generally in one phase under X-ray resolution, is the main characteristic of this ceramic. However, the presence of secondary phases in the microstructure of SnO_2-based varistors has been recently reported [8,10].

The effects on the global properties of SnO_2 varistors of Co_3O_4, CoO, ZnO, Sb_2O_3, Nb_2O_5, Fe_2O_3 and La_2O_3, among other metal oxides, have been systematically studied. It has been determined that Co, Mn and Zn oxides create charged oxygen vacancies at sintering temperatures that enhance diffusion and mass transport mechanisms leading to densification and grain growth. Conversely, Sb_2O_3 and Nb_2O_5 decrease the sintering rate of SnO_2 when forming solid solution and increase the electrical conductivity. Moreover, trivalent metal oxides (Fe_2O_3, La_2O_3, Al_2O_3 and Pr_2O_3) have been found to improve the non-linear properties of SnO_2-based varistors [10–13].

In this work, the effect of the addition of Y_2O_3 on the microstructure and on the electrical properties of the $SnO_2{\cdot}Co_3O_4{\cdot}Nb_2O_5$ (SCN) varistor system was studied. This is an oxide whose cation has a similar ionic radius to that of La^{3+} which has proven to be an excellent enhancer of the non-linear properties; thus, yttria might as well form solid

* Corresponding author. Tel.: +54 223 4816600; fax: +54 223 4810046.
E-mail address: rparra@fi.mdp.edu.ar (R. Parra).

0254-0584/$ – see front matter © 2005 Published by Elsevier B.V.
doi:10.1016/j.matchemphys.2005.05.014

Table 1
Sample composition (mol%)

	SnO_2	Co_3O_4	Nb_2O_5	Y_2O_3
SCN	99.62	0.33	0.05	–
SCN–0.05Y	99.57	0.33	0.05	0.05
SCN–0.10Y	99.52	0.33	0.05	0.10
SCN–0.25Y	99.37	0.33	0.05	0.25

solution and contribute to the formation of effective voltage barriers.

2. Experimental procedure

Analytical grades of SnO_2 (Aldrich, 99.9%), Co_3O_4 (Merck, >99%), Nb_2O_5 (Fluka AG, 99.9%), and Y_2O_3 (Sigma, 99.9%) were used as precursors for SnO_2-based varistors. Selected compositions are listed in Table 1. Oxides were mixed in 2-propanol stirring in a high-speed turbine at 6000 rpm for 5 min and subsequently dried at 65 °C for 48 h. Then, mixtures were crushed into powders and sieved through a 43 μm mesh screen. Discs of a thickness around 1 mm were prepared by uniaxial pressing of the powders at 150 kg cm^{-2}. The obtained pellets were sintered in a stationary air atmosphere at 1300 °C for 2 h with heating and cooling rates of 3 °C min^{-1} in a Carbolite RHF17/6S furnace.

The apparent density of sintered samples was determined through the Archimedes method. X-ray diffraction analysis (XRD) was carried out by means of a Philips 1830/00 diffractometer running with Co Kα radiation at 40 kV and 30 mA. The microstructures were characterized by scanning electron microscopy (SEM) in a Topcon SM-300 microscope under the secondary electrons mode, and by transmission electron microscopy (TEM) in a Philips CM200 instrument operating at 200 kV. Both SEM and TEM instruments were equipped with EDS systems for energy dispersive X-ray analysis.

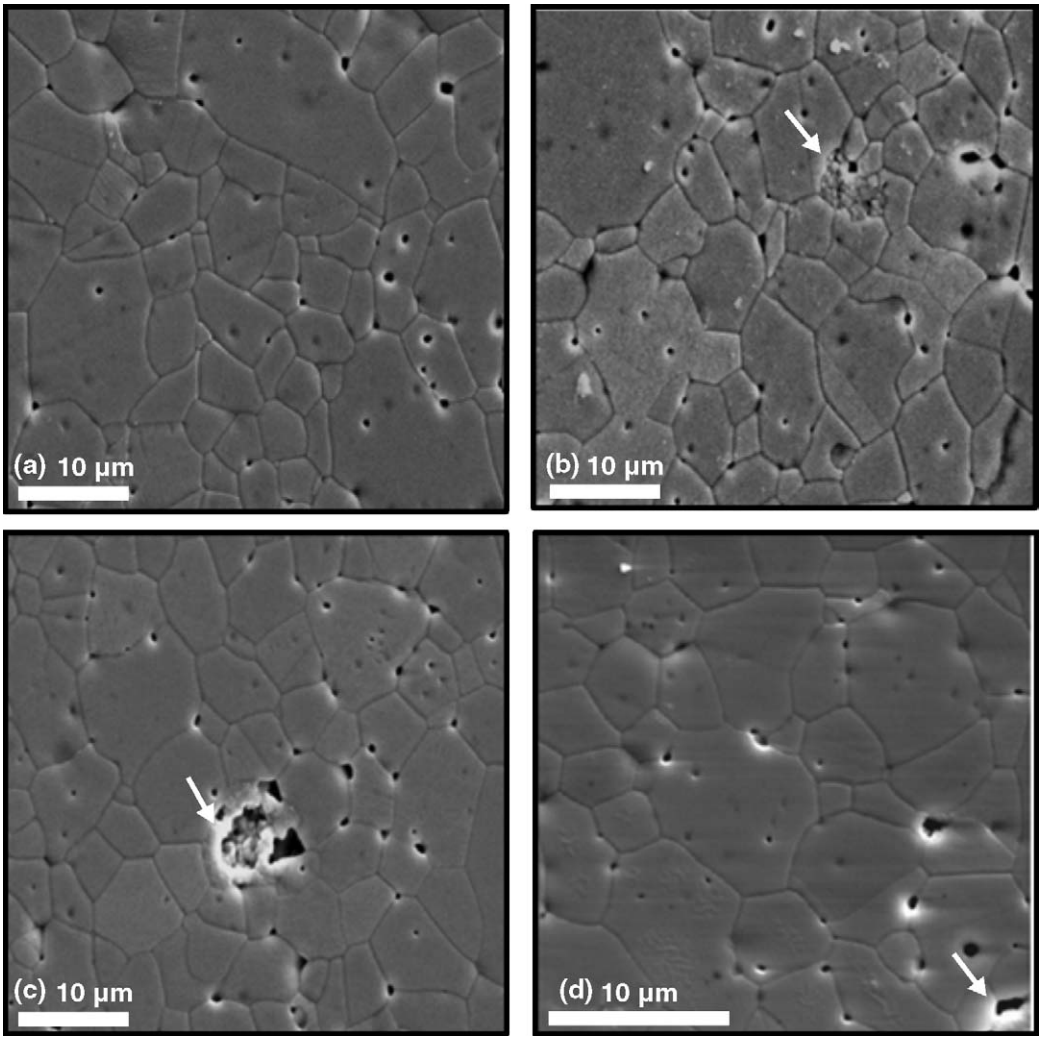

Fig. 1. SEM images of the compositions under characterization: (a) SCN, (b) SCN–0.05Y, (c) SCN–0.10Y and (d) SCN–0.25Y. Agglomerated particles of a secondary phase are arrowed.

Table 2
Percentage of theoretical density (ρ_t), average grain size (d), electric breakdown field (E_r), non-linearity coefficient (α) and barrier voltage (V_b) for samples sintered at 1300 °C for 2 h

	$\%\rho_t$	d (μm)	E_r (V cm^{-1}) at 1 mA cm^{-2}	E_r (V cm^{-1}) at 10 mA cm^{-2}	α	V_b (V barrier^{-1}) at 10 mA cm^{-2}
SCN	98.2	5.8	2100	2490	14	1.4
SCN–0.05Y	97.3	5.2	2830	3270	16	1.5
SCN–0.10Y	97.0	4.7	1830	2760	6	0.9
SCN–0.25Y	96.8	4.6	1610	2880	4	0.7

SnO_2 theoretical density = 6.95 g cm^{-3}; band gap = 3.5 eV.

Samples for SEM were polished and thermally etched 50 °C below the sintering temperature. Average grain sizes were determined through the method of the intercepts [14]. Suitable samples for TEM were prepared by cutting discs of plane and parallel faces of 3 mm in diameter using an ultrasonic cutter. The discs were grinded down to a thickness of 100 μm and then dimpled by means of an SBT Dimple Grinder Model 515 to get a 30 μm thickness at the centre of the specimens. Finally, large electron transparent regions were achieved by ion milling performed in a Bal-Tech RES010 ion mill operating at 4 kV and 1.5 mA on each gun.

Electron diffraction patterns were obtained from selected areas. The relationship in a diffraction pattern

$$Rd = \lambda L, \quad (1)$$

where R is any distance measured on the pattern related to a specific d spacing in the lattice and λL the microscope constant, was applied for phase identification [15].

Silver electrodes were painted on the plane surfaces of sintered samples for electrical characterization. A Keithley 237 high voltage source-measure unit was used to obtain the current density versus electric field characteristics at room temperature.

3. Results and discussion

Fig. 1 shows the developed microstructures and Table 2 presents the densities and average grain sizes measured for each sample. Yttria addition to the SCN system caused a decrease both in density and mean grain size; moreover, these properties decreased even more with subsequent additions of Y_2O_3. As seen in the micrographs, samples with yttrium developed clusters of crystals of a secondary phase that might be interfering with grain growth and densification of the material. Fig. 2 shows the EDS analysis over a region with a cluster of precipitates as observed with SEM. Only Sn and O were detected in the grains, whereas also Y is present in the precipitates. Curiously, no other additive showed up in the analysis even though compounds such as Co_2SnO_4 have been reported to occur in similar systems being 1 mol% in Co [8–10]. Precipitates including Nb were neither detected with SEM in previous works [10]. Therefore, it is assumed that Co_3O_4 and Nb_2O_5 are well distributed within the lattice and their local concentrations are below the detection limits of the equipment used.

Further microstructural characterization was accomplished through EDS assisted TEM. The image in Fig. 3

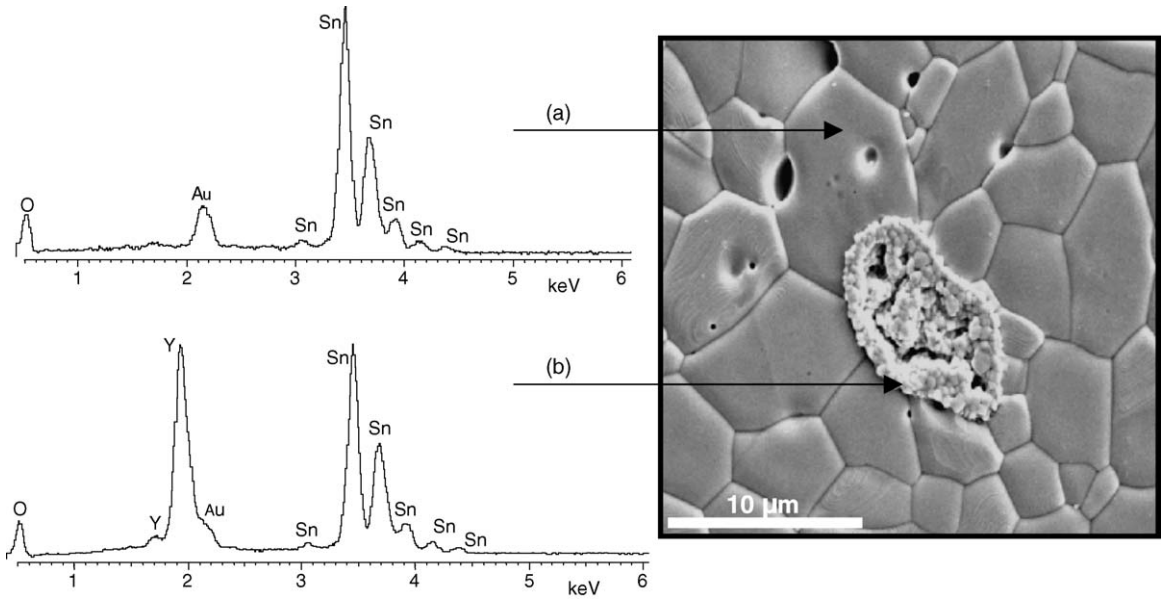

Fig. 2. SEM image of the SCN–0.05Y system showing a cluster of particles of a secondary phase, and EDS analysis of: (a) grain region and (b) precipitates.

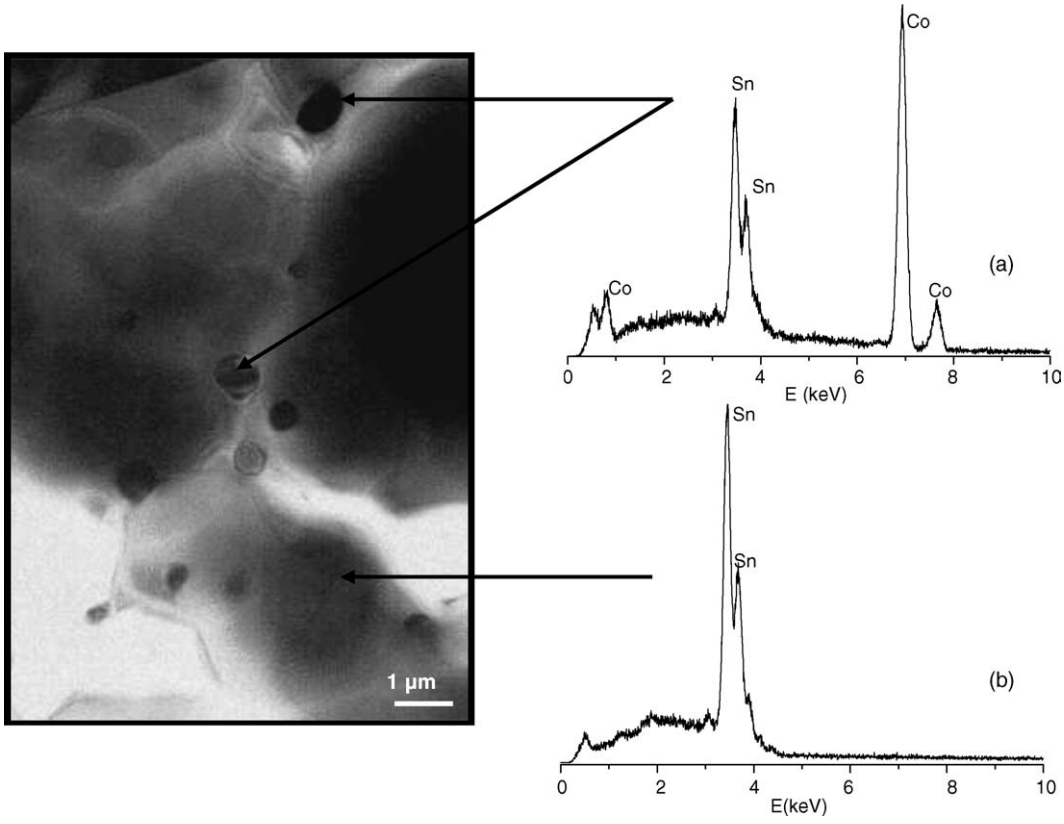

Fig. 3. TEM image and EDS analysis of: (a) precipitates of a secondary phase in the boundary of two grains and (b) of the grain region in the SCN–0.05Y system.

shows precipitates smaller than 1 μm in diameter located in the limits of two SnO_2 grains. In contrast with the composition of the precipitates found with SEM where Y is present, these particles are composed of Sn, Co and O. The acquisition of the SAD patterns in Fig. 4 allowed to phase identification; Fig. 4a corresponds to the matrix of SnO_2, whereas the pattern in Fig. 4b was indexed as the cubic phase ($a = 8.637$ Å) Co_2SnO_4 (JCPDS 29-0514).

Phase composition was also examined by means of X-ray diffraction analysis. The powder patterns displayed in Fig. 5 were registered between 30 and 40° (2θ) to give attention to the signals of those phases different from SnO_2. The peak around 35.5° (2θ) corresponds to SnO, phase present in every system that arises due to the atmospheric conditions during sintering. The peak in the vicinity of 34.5° that showed up in the SCN–0.10Y system, is attributed to the (2 2 2) reflection

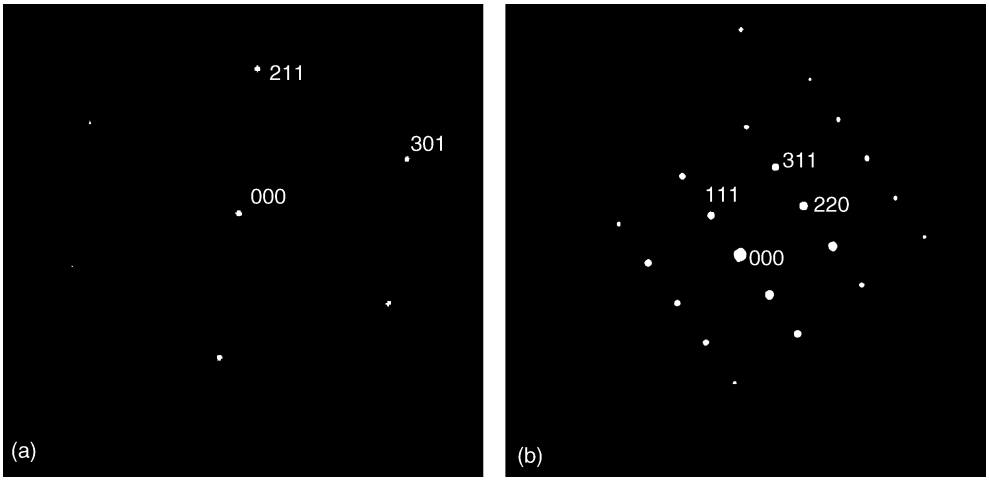

Fig. 4. (a) SAD pattern of the grain region matching for SnO_2 and (b) SAD pattern of a precipitate matching for a well crystallized Co_2SnO_4-phase in sample SCN–0.05Y.

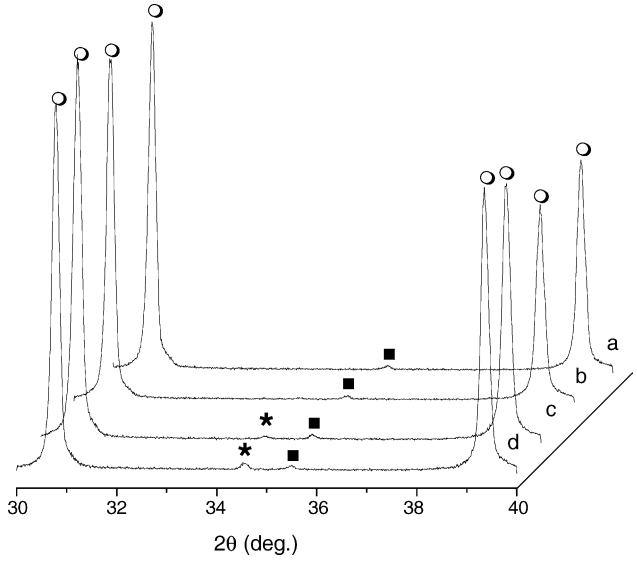

Fig. 5. XRD-powder patterns of samples: (a) SCN, (b) SCN–0.05Y, (c) SCN–0.10Y and (d) SCN–0.25Y sintered at 1300 °C for 2 h showing the different identified phases. (◯) SnO_2; (■) SnO; (*) $Y_2Sn_2O_7$.

of the cubic phase $Y_2Sn_2O_7$ (JPCDS 73-1684) in agreement with the results obtained through EDS and suggesting that Y^{3+} does not occupy Sn-sites in the lattice. The fact that detecting the $Y_2Sn_2O_7$ phase is possible with XRD indicates that most of yttria is reacting with SnO_2 to yield agglomerates of precipitates such as those observed in Figs. 1 and 2. Rare earth stannates pyrochlore oxides, $Ln_2Sn_2O_7$ (Ln = Y, La–Lu), are a well-known group of isostructural compounds [16,17]. The chemical affinity between Sn and Y seems to prevail over solid solution formation, which is disfavored due to the 30% difference that exists between their ionic radii ($r_Y^{3+} = 0.93$ Å; $r_{Sn}^{4+} = 0.71$ Å).

The effect of precipitates on the electrical properties of SnO_2-based varistors has been studied but is not yet completely understood; however, their negative effects have been systematically exposed [8–10]. The effect of adding a 0.05 mol% of Y_2O_3 to the SCN system was to increase, though slightly, both the electric breakdown field (E_r) and the non-linearity coefficient α (Table 2). The observed increase in E_r may be ascribed to the higher number of effective potential barriers due to the smaller grains of the yttrium-doped sample. The electrical properties were negatively modified with subsequent additions of yttria as Fig. 6 and Table 2 show. The non-linearity coefficient decreased from 16 to 4 from sample SCN–0.05Y to sample SCN–0.25Y. Even though the mean grain size followed a decreasing trend, the E_r also dropped, indicating that the electrical properties and conduction mechanisms are being somehow altered. The grain boundary breakdown voltage (V_g) in a sample of thickness L and mean grain size d can be estimated as

$$V_g = \frac{E_r d}{L}. \quad (2)$$

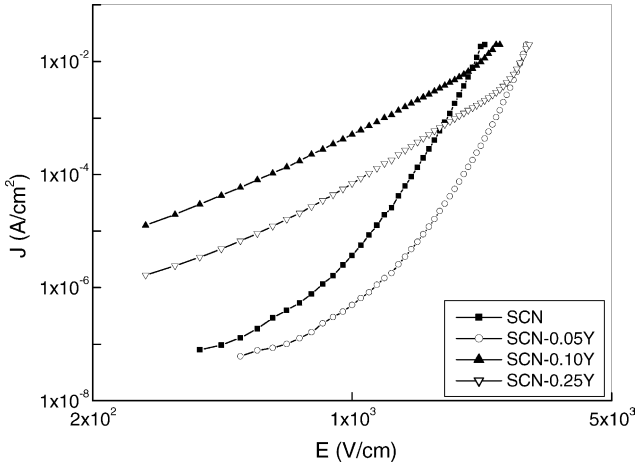

Fig. 6. Current density (J) vs. electric field (E) curves registered at 25 °C.

An increase in V_g is observed (Table 2) with the addition of 0.05 mol% of Y_2O_3 to the SCN sample; however, its value greatly diminishes after increasing the percentage of Y_2O_3 to 0.10 and 0.25. Assuming the grain boundary breakdown value as compatible with the SnO_2 band gap of 3.5 V, the number of effective potential barriers increases from 41 to 42% of the total number of grain boundary barriers for sample SCN–0.05Y respect to sample SCN. For samples with 0.10 and 0.25 mol% of yttria, the number of effective barriers falls to 24 and 21%, respectively. It seems that the likelihood of Y^{3+} species to precipitate into pyrochlore phases damages the electrical response of the devices by decreasing the number of effective voltage barriers.

4. Conclusions

The experimental results reported in this paper lead to the understanding of the influence of Y_2O_3 on the microstructure development and on the electrical properties of SnO_2-based varistors. Secondary phases other than SnO_2 have been identified through different characterization techniques. Particles of Co_2SnO_4 were observed at grain–grain interfaces within TEM magnification. The occurrence of agglomerates of particles of $Y_2Sn_2O_7$ has been determined to inhibit grain growth and material densification. The electrical properties were severely damaged after increasing the amount of Y_2O_3 from 0.05 to 0.25 mol%; the effective potential barriers were seen to decrease with the addition of yttria. A satisfactory composition of $99.57SnO_2$–$0.33Co_3O_4$–$0.05Nb_2O_5$–0.05 mol% Y_2O_3 with the highest non-linearity ($\alpha = 16$) was obtained.

Acknowledgements

The authors express their thanks to the Programa CIAM, to CONICET (Argentina), to CNPq and FAPESP (Brazil) for their financial support.

References

[1] T.K. Gupta, J. Am. Ceram. Soc. 73 (1990) 1818.
[2] M. Matsuoka, Progress in research and development of zinc oxide varistors, in: L.M. Levinson (Ed.), Grain Boundary Phenomena in Electronic Ceramics, Advances in Ceramics, vol. 1, The American Ceramic Society Inc., Ohio, 1981, pp. 290–308.
[3] L.M. Levinson, H.M. Philipp, Am. Ceram. Soc. Bull. 65 (1986) 639.
[4] Z. Brankovic, G. Brankovic, D. Poleti, J.A. Varela, Ceram. Int. 27 (2001) 115.
[5] C.H. Kim, J.H. Kim, J. Eur. Ceram. Soc. 24 (2004) 2537.
[6] M.S. Castro, C.M. Aldao, J. Eur. Ceram. Soc. 17 (1997) 1533.
[7] S.A. Pianaro, P.R. Bueno, E. Longo, J.A. Varela, J. Mater. Sci. Lett. 14 (1995) 692.
[8] M.M. Oliveira, P.C. Soares Jr., P.R. Bueno, E.R. Leite, E. Longo, J.A. Varela, J. Eur. Ceram. Soc. 23 (2003) 1875.
[9] L.P.G. Simoes, P.R. Bueno, M.O. Orlandi, E.R. Leite, E.R. Longo, J. Electroceram. 10 (2003) 63.
[10] R. Parra, M.S. Castro, J.A. Varela, J. Eur. Ceram. Soc. 25 (2004) 401.
[11] J. Fayat, M.S. Castro, J. Eur. Ceram. Soc. 23 (2003) 1585.
[12] J.F. Wang, Y.J. Wang, W.B. Su, H.C. Chen, W.X. Wang, Mater. Sci. Eng. B 96 (2002) 8.
[13] S.R. Dhage, V. Ravi, S.K. Date, Mater. Lett. 57 (2002) 727.
[14] M.I. Mendelson, J. Am. Ceram. Soc. 52 (1969) 443.
[15] D.B. Williams, C.B. Carter, Transmission Electron Microscopy: A Text Book for Materials Science, Plenum Press, New York, 1996.
[16] B.J. Kennedy, B.A. Hunter, C.J. Howard, J. Solid State Chem. 130 (1997) 58.
[17] Z. Lu, J. Wang, Y. Tang, Y. Li, J. Solid State Chem. 177 (2004) 3075.